Published in final edited form as:
Psychopharmacology (Berl). 2012 June ; 221(3): 479–492. doi:10.1007/s00213-011-2595-7.

Suppression of endogenous PPARγ increases vulnerability to methamphetamine –induced injury in mouse nigrostriatal dopaminergic pathway

Seong-Jin Yu, **Mikko Airavaara**, **Hui Shen**, **Jenny Chou**, **Brandon K. Harvey**, and **Yun Wang**
National Institute on Drug Abuse, IRP

Abstract

Rationale—Methamphetamine is a commonly abused drug and dopaminergic neurotoxin. Repeated administration of high doses of methamphetamine induces programmed cell death, suppression of dopamine release, and reduction in locomotor activity. Previous studies have shown that pretreatment with Peroxisome Proliferator-Activated Receptor gamma (PPARγ) agonist reduced Methamphetamine -induced neurodegeneration.

Objectives—The purpose of this study was to examine the role of endogenous PPARγ in protecting against methamphetamine toxicity.

Methods—Adeno-associated virus (AAV) encoding the Cre recombinase gene was unilaterally injected into the left substantia nigra of loxP-PPARγ or control wild type mice. Animals were treated with high doses of methamphetamine 1-month after viral injection. Behavioral tests were examined using Rotarod and rotometer. In vivo voltammetry was used to examine dopamine release/clearance and at 2 months after methamphetamine injection.

Results—Administration of AAV-Cre selectively removed PPARγ in left nigra in loxP-PPARγ mice but not in the wild type mice. The loxP-PPARγ/AAV-Cre mice that received methamphetamine showed a significant reduction in time on the rotarod and exhibited increased ipislateral rotation using a rotometer. The peak of dopamine release induced by local application of KCl and the rate of dopamine clearance were significantly attenuated in the left striatum of loxP-PPARγ/AAV-Cre animals. Tyrosine hydroxylase immunoreactivity was reduced in the left, compared to right, nigra and dorsal striatum in loxP-PPARγ/AAV-Cre mice receiving high doses of methamphetamine.

Conclusion—A deficiency in PPARγ increases vulnerability to high doses of methamphetamine. Endogenous PPARγ may play an important role in reducing methamphetamine toxicity in vivo.

Introduction

Peroxisome Proliferator-Activated Receptor gamma (PPARγ) is a nuclear receptor which forms a complex with the retinoic X receptor (RXR) and binds to the PPAR response element (PPRE) in the promoter region of specific genes, such as interleukin -1β, IL-6, TNF-α, catalase, and superoxide dismutase to regulate their expression. PPARγ is also present in cytosol in neuronal cells (Isaac et al., 2006; Xu et al., 2010) and can be translocated to nuclei after injury (Xu et al., 2010). PPARγ is involved in attenuating

Address for correspondence: Yun Wang, M.D., Ph.D., National Institute on Drug Abuse, I.R.P., Neural Protection and Regeneration Section, 251 Bayview Boulevard, 06-721A, Baltimore, MD 21224, TEL: 443-740-2587 FAX: 443-740-2840, ywang@intra.nida.nih.gov.

neurodegeneration in several neurological diseases, including Parkinson's disease (Dehmer et al., 2004; Schintu et al., 2009), Alzheimer's disease (Jiang et al., 2008), and stroke (Shimazu et al., 2005; Tureyen et al., 2007; Victor et al., 2006; Zhao et al., 2005) as well as methamphetamine (MA)- induced psychomotor sensitization (Maeda et al., 2007).

MA is a commonly abused drug and dopaminergic neurotoxin. Repeated administration of high doses of MA induces programmed cell death, suppression of dopamine (DA) release, and reduction in tyrosine hydroxylase (TH) immunoreactivity. Some of these pre-synaptic changes are reversible. Using an *in vivo* electrochemical measurement, it has been shown that potassium-evoked DA overflow in striatum was reduced 1 week after high dose MA administration in adult Fisher rats. The evoked DA overflow partially recovered after 1 month and fully recovered by 6 months (Cass and Manning, 1999). These data suggest that high doses of MA can induce a reversible electrochemical dysfunction in dopaminergic neurons.

Recent studies have indicated that PPARγ agonists can modify neurodegeneration in dopaminergic neurons. Chronic treatment with the PPARγ agonists rosiglitazone or piloglitazone attenuated MPTP-mediated motor deficits and loss of TH(+) cells in substantia nigra pars compacta in mice (Quinn et al., 2008; Schintu et al., 2009). Administration of rosiglitazone reduced microglial activation and partially restored dopamine content in MPTP -lesioned animals (Schintu et al., 2009). Pretreatment with the PPARγ agonist 15d-PG J2 or ibuprofen reduced the high dose MA -mediated loss of DAT immunoreactivity and the accumulation of microglial cells in the striatum 3 days after repeated MA injection (Tsuji et al., 2009). Taken together, these data suggest that activation of PPARγ reduces neurodegeneration induced by MA or other dopaminergic toxins. The endogenous protective role of PPARγ pathway against dopaminergic toxins, i.e. in the absence of pharmacological agonists, is still not fully clarified, particularly since the agonists used may have actions at other sites.

The purpose of this study was to examine the protective roles of endogenous PPARγ in MA –mediated neurodegeneration using PPARγ deficient animals. The conventional elimination of PPARγ in knock-out mice results in early lethality by embryonic day 10–11 due to placental dysfunction (Barak et al., 1999). The Cre/loxP system can be used to produce a cell-specific or conditional knockout by deleting a gene of choice in a specific cell type. In this study, we selectively removed PPARγ in the substantia nigra unilaterally by stereotaxic injection of an adeno-associated virus (AAV) encoding the gene for Cre recombinase, which resulted in excision of the PPARγ gene coding sequence flanked by loxP sites (Kaspar et al., 2002; Scammell et al., 2003). We found that a deficiency of PPARγ in the substantia nigra increases vulnerability to high doses of MA.

Methods

AAV vectors

The generation of the control vector, AAV-GFP (green fluorescent protein), has been described elsewhere (Lowery et al., 2009). The construction of AAV-GFP/Cre (Cre-GFP fusion protein, referred to as "AAV-Cre" in the current manuscript) has also been described previously (Kaspar et al., 2002). Viral stocks were prepared using a triple transfection method (Howard et al., 2008; Xiao et al., 1998). Both vectors were packaged using pAAV7, the rep/cap plasmid for generating serotype 7 (Gao et al., 2002). Plasmids used for packaging AAV were generously provided by Dr. Xiao Xiao (UNC, Chapel Hill, NC). Both vectors were purified by CsCl gradient and titered by quantitative PCR using GFP as the target sequence. Viral titers are recorded as viral genome/mL.

Animals

Homozygous loxP-PPARγ mice (Strain Name: B6.129-Ppargtm2Rev/J; Stock Number: 004584) were purchased from Jackson laboratories and were bred in the animal facility at the NIDA IRP. Control wild type (WT) mice (C57/BL6) were purchased from CRL laboratories. All protocols and animal care procedures were in accordance with the National Institute of Health Guide for the Care and Use of Laboratory Animals (NIH Publications No. 80-23, revised 1996). The use of these animals for this study was approved by the Animal Care and Use Committee, NIDA. All animals were genotyped by PCR before viral injection according to previously described methods (He et al., 2003).

Unilateral AAV injection into substantia nigral region

Adult male loxP-PPARγ and WT mice were anesthetized with chloral hydrate (400 mg/kg, i.p.). The animals were placed in a stereotaxic frame (Stoelting), where a 10 μl Hamilton syringe with a 30 gauge needle was used to stereotactically deliver AAV-Cre (2 μl of 5×10^9 viral genomes/μl) at a speed of 0.5 μl/min into left substantia nigral region (coordinates: AP −3.3 mm, ML +1.2 mm to bregma and DV 4.2 mm from skull surface according to Paxinos and Franklin's "the Mouse Brain"). The needle remained in the brain for 2 minutes after the injection then slowly removed. After recovery from anesthesia, animals were housed in their home cages.

Injection of MA or saline

At one month after viral injection, animals were treated with (+) MA (10 mg/kg, × 4 doses, each dose two hours apart) or saline (every 2 hours, 4 doses, s.c.). This high dose of MA is required to induce neural toxicity in rodents (Grace et al., 2010; Jayanthi et al., 2005; Zhu et al., 2006) and has been used to examine protection against MA –mediated neural degeneration in mice (Chou et al., 2008; Wang et al., 2001). Core body temperature was monitored by a mouse rectal probe (YSI, Yellow Springs, OH).

Rotarod treadmill test

Animals received 3 days of training (twice daily) before MA or saline administration. Each animal was placed in the respective lane on treadmill, 13.75 inches above the testing platform. For training, the rod was rotated at 5 rpm initially and then accelerated to 10 rpm. The test was performed again at 10 rpm on days 3, 10, 42 after MA or saline injection. Cut-off time for each test was 360 sec. Each animal was tested 5 times per day. The two longest endurance times (ETime) on the rotating rod in 5 trials were averaged and used for analysis.

Rotation

At 45 days after MA or saline injection, animals were tested for rotational behavior in response to subcutaneous (+) MA injections (2.5 mg/kg, s.c.) in an automated rotometer (Accuscan Instruments, Columbus, Ohio). Each animal was placed in a cylindrical test chamber for 90 min. The highest consecutive clockwise and counter-clockwise rotations over 60- min were used for analysis.

Western blot analysis

The frozen striatal tissues were homogenized in RIPA buffer containing 50mM Tris HCl pH 7.4,1% NP40,0.25% Deoxycholic Acid, 150 mM sodium chloride,1mM EDTA and1% Protease inhibitor (Roche, Germany). Lysates were cleared by centrifugation (14,000g at 4 °C for 5 min), and the total protein concentration in each sample was determined by DCA assay using bovine serum albumin (BSA) as a standard curve. Lysates were separated by NuPAGE®Novex Bis-Tris Gels4-12% Gel from Invitrogen and the proteins were transferred to Immobilon-FL membranes (Millipore, Billerica, MA). After pre-blocking in

Odyssey blocking buffer from Li-Cor for overnight at 4 °C, the membranes were incubated with the primary antibody to Rabbit anti- Actin (1:2500, Sigma, ST Louis, MO) and Mouse anti-TH (1:5000, Millipore) at room temperature for two hours, then incubated for hour and half in Goat anti-rabbit IR-700nm, Goat-anti-mouse IR-800nm secondary antibodies (1:2500, Li-Cor, Lincoln, NE, USA). The membranes were scanned using an Odyssey Infrared Imager (Li-Cor, Lincoln, NE, USA). Immunoblots were quantified with ImageJ.

In vivo voltammetry

KCl –evoked DA release in striatum was measured at >2 months after MA or saline injection. Animals were anesthetized using urethane (1.25 g/kg, i.p.). In-vivo chronoamperometric measurements of extracellular dopamine (DA) concentration were performed as previously described (Zhou et al., 1996). The recordings were taken at rates of 10 Hz continuously using Nafion-coated carbon-fiber working electrodes (tip = 30 μm; SF1A, Quanteon, Lexington, Kentucky) and a microcomputer-controlled apparatus (FAST system, Quanteon). The release of DA was measured by changes of extracellular DA concentration after microinjection of KCl into the striatal parenchyma. KCl (70 mM) in osmolarity balanced saline (79 mM NaCl and 2 mM $CaCl_2$) was locally applied through a micropipette at 100 to 200 nl range. The concentration and volume of KCl solution in the pipette have been previously reported to induce depolarization and release of dopamine at dopaminergic nerve terminals in vivo (Hoffman et al., 1998; Wang et al., 2003). The working electrode and the micropipette were mounted together with sticky wax; tips were separated by 150 μm. The electrode/pipette assembly was lowered into striatum (AP 0–0.5 mm, M/L 2.0 mm relative to bregma and 1.5 to 3.5 mm below the dura). Local application of KCl from the micropipette was performed by pressure ejection using a pneumatic pump (BH2, Medical System). The ejected volume was monitored by recording the change in the fluid meniscus in the pipette before and after ejection using a dissection microscope.

Immunohistochemistry

Mice were perfused transcardially with saline followed by 4% paraformaldehyde (PFA) in 0.1 M PBS. Brains were stored in 18% sucrose and sectioned coronally (25 μm) using a Leica cryostat. Free-floating brain sections were rinsed three times with phosphate buffer (PB) for 10 min and incubated for 1h with blocking solution (4% BSA and 0.3% Triton X-100 in PB). Brains sections (25 μm in thickness) were immunolabeled using primary anti-tyrosine hydroxylase (TH) polyclonal antibody (Millipore, Temecula, CA; 1:500) for 2 days or rabbit anti-PPARγ (Santa Cruz biotechnology, Santa Cruz, CA; 1:50) antibody overnight at 4°C. For immunofluorescence, molecular probes Alexa 568 secondary antibodies (Invitrogen, Carlsbad, CA; 1:500) were included for 3 days for TH or overnight at 4°C for PPARγ. Nuclei were counterstained with 4', 6-diamidino-2-phenylindole (DAPI; Molecular Probes, 1:1000). Control sections were incubated without primary antibody. Confocal analysis was performed using Nikon D-ECLIPSE 80i microscope and EZ-C1 3.90 software.

Quantification of TH immunoreactivity in striatum

The bound primary antibody primary anti-tyrosine hydroxylase (TH) polyclonal antibody (Millipore, Temecula, CA; 1:500) was visualized using the infrared-labeled secondary antibody (goat anti-Rabbit IRDye800, Rockland Immunochemicals Inc.) 1:500 in 4% BSA and 0.3% Triton X-100 in PB for 1 h. Sections were rinsed three times with PB and mounted on gelatin/chrome-alum coated slides and coverslipped. TH immunoreactivity in brain sections were scanned and quantified by a Li-Cor Odyssey Scanner. TH signal from cerebral cortex was used as a background and subtracted from striatum TH signal. Densitometry was carried out in sections with an identified anterior commissure (between AP: +1.10 mm ~ 0.14 mm to bregma) and signals were averaged.

TH cell count in midbrain

An ABC method was used and sections were incubated in biotinylated horse anti-rabbit IgG (1:200; Vector Laboratories, Burlingame CA) for 1 h, followed by incubation for 1 h with avidin-biotin-horseradish peroxidase complex as described previously (Chou et al., 2008). Staining was developed with 2, 3′-diaminobenzidine tetrahydrochloride (0.5 mg/mL). Sections were then mounted on gelatin/chrome-alum coated slides and coverslipped. For TH positive cell counts histological images were acquired using an Infinity 3 camera, NIKON 80i microscope and QCapture Pro 5.0 software and TH positive cell counts were done with NIS elements software (Nikon) and personnel blinded as to treatment. TH positive cells were averaged from sections between AP: −3.16 mm ~ −3.64 mm to bregma as described previously (Chou et al., 2008).

RNA isolation and standard PCR for detection of recombination

Approximately 2 weeks after injection, animals were euthanized and brains removed. Using a cryostat, brains were coronally sectioned from posterior to anterior from 1 mm posterior to the site of injection and a 2 mm diameter tissue punch (~2 mm depth) was made from each hemisphere and combined. Total RNA was isolated from the combined hemispheres using Rneasy Lipid Extraction Kit (Qiagen) and revere transcribed using iScript cDNA synthesis kit (Biorad). Using established reaction conditions and primers (Zhao et al., 2009), PCR was performed to detect wild-type (700 bp) and recombinant PPARγ (300 and 400 bp). Quantitative PCR: Using cDNA prepared as described above, PPARγ and ubiquitin-conjugating enzyme E2I (Ube2i, reference gene) mRNA levels were measured by real-time quantitative PCR (TaqManTM chemistry, Roche) and analyzed with an CFX96 thermal cycler (Bio-Rad). PPARγ and Ube2i primers and probes were designed using Real Time Design (Bioresearch Technologies, Novato, CA). UBE2i was used as a housekeeping gene based on previous work (Kobayashi et al., 2004). Real-time PCR results were calculated using the 2 - ΔΔCT method (Schmittgen and Livak, 2008). Briefly, the threshold cycle (Ct) of PPARγ was normalized to the Ct of the reference gene Ube2i for each sample, which was used to determine fold changes in PPARγ mRNA expression compared to wild-type animals injected with AAV-GFP.

Primer and probe sequences are as follows:

PPARγ: 5’ GCCCTTTACCACAGTTGATTTCTC 3’(fwd),

5’FAM- TTCTGCTCCACACTATGAAGACATTCCA -BH1 3’ (probe),

5’ GCAACCATTGGGTCAGCTCTT 3’ (rev),

Ube2i: 5’GCCACCACTGTTTCATCCAAA3’ (fwd),

5’FAM-CGTGTATCCTTCTGGCACAGTGTGC-BH1 3’ (probe),

5’GCCGCCAGTCCTTGTCTTC3’ (rev).

Results

AAV-Cre and recombination of loxP-PPARγ

A total of 12 loxP-PPARγ and 12 wild type mice received intranigral administration of AAV-Cre (serotype 7) or AAV-GFP. Recombination by AAV-Cre was confirmed by standard PCR of cDNA prepared from tissue punches of midbrain at 2 weeks after viral delivery. Only loxP-PPARγ animals that received AAV-Cre were positive for recombination (Fig 1A). Quantitative PCR analysis of the cDNA from the midbrain showed a 50% reduction ($p=0.0019$, $F_{(3, 23)}= 7.123$, One way ANOVA + Newman-Keuls test) in PPARγ mRNA levels for loxP-PPARγ animals receiving AAV-Cre, compared to all other

groups (Fig 1B). The efficiency of AAV serotype 7 transduction was examined 2 weeks after local administration of AAV-Cre in 3 WT mice. AAV transduced about 56 ± 4% of TH cells in the nigra based on colocalization of TH-immunoreactivity and GFP fluorescence (Fig 1C–E). Overall, these results demonstrate that AAV-GFP/Cre successfully transduced dopaminergic neurons and caused a reduction in PPARγ expression in the nigra region.

At 1 month after AAV injection, the GFP fluorescence from the GFP/Cre fusion of AAV-Cre was expressed in TH and non-TH cells in left nigra region (Fig 2). Using confocal microscopy, we found that GFP fluorescence co-localized with the nuclear marker DAPI in the TH neurons (Fig 2D). No GFP fluorescence was found in the striatum or in the contralateral hemisphere. These data suggest that Cre-GFP fusion protein was produced in the dopaminergic and non-dopaminergic cells at the site of injection and localized to the nucleus. Immunolabeling cells in the substatia nigra for PPARγ showed a decrease of PPARγ-immunoreactivity in GFP/Cre-positive cells of loxP-PPAR, but not wild-type, animals (Fig 3).

TH Immunoreactivity in striatum

WT and loxP-PPARγ mice were treated with AAV-Cre unilaterally in left nigra area. Striatal tissue in left hemisphere was collected for Western analysis at 2 days after MA or saline administration. MA treatment, compared to saline treatment, significantly reduced striatal TH/actin immunoreactivity in loxP-PPARγ/AAV-Cre and WT/AAV-Cre mice ($p<0.05$, $F_{1,33}=22.349$, two way ANOVA +post-hoc Newman-Keuls test, Fig 4A and B). Our data suggest that high doses of MA can acutely induce neurodegeneration in striatum. No difference was found in striatal TH activity between loxP-PPARg /AAV-Cre and WT/AAV-Cre mice receiving MA. These data suggest that MA induces a similar neurodegeneration in these mice at 2 days after MA treatment.

Rotarod

A total of 34 mice (15 loxP-PPARγ and 19 WT mice) were treated with AAV-Cre unilaterally in left nigra area. Animals received 3 days of training before MA or saline administration. One WT mouse was removed from this behavioral study during the training period. One month after viral injection, animals were treated with MA (n=15) or saline (n=18). Rotorod tests, at 10 rpm, were taken on day 3, 10 and 42 after injection of MA or saline. Saline injection did not alter the endurance time (Etime) in loxP-PPARγ/AAV-Cre and WT/AAV-Cre mice (Fig 5). In contrast, high doses of MA significantly reduced Etime up to 42 days after injection ($F_{1,84}=102.337$, $p<0.001$, three way ANOVA). There is a statistically significant interaction between the administration of MA and treatment of AAV-Cre in loxP-PPARγ animals ($F_{1,84}=5.286$, $p=0.024$, three way ANOVA, Fig 5), suggesting that unilaterally deleting PPARγ potentiates MA –mediated behavioral deficits. Post-hoc Newman-Keuls analysis indicates a significant reduction of Rotarod performance in loxP-PPARγ mice treated with AAV-Cre and MA, compared to WT mice treated with AAV-Cre and MA ($p=0.012$).

Rotation

A two-way ANOVA was used to analyze rotational behavior in 34 mice at 45 days after receiving saline or MA (10 mg/kg ×4). Rotation was recorded every two minutes for 90 min after administration of a low dose of MA (2.5 mg/kg, s.c.). Animals developed both ipislateral and contralateral rotation after injection. No difference was found in the contralateral rotation between loxP-PPARγ/AAV-Cre and WT/AAV-Cre mice ($F_{1,29}=0.002$, $p=0.963$, Fig 6B), or treatment with saline or high dose MA ($F_{1,29}=0.002$, $p=0.963$). In contrast, there is a significant difference in ipislateral rotation between loxP-PPARγ/AAV-Cre and WT/AAV-Cre mice ($F_{1,29}=12.366$, $p=0.01$). There is also a

significant interaction between use of MA and treatment with AAV-Cre in loxP-PPARγ mice($F_{1,29}$=5.288, p=0.029). Post hoc Newman-Keul test indicates that treatment with high dose of MA significantly increased ipislateral rotation in loxP-PPARγ/AAV-Cre animals, as compared to WT/AAV-Cre controls (p<0.05, Fig 6A).

KCl-induced DA release in striatum

KCl-evoked DA release in striatum was examined using in vivo voltammetry in 8 loxP-PPARγ/AAV-Cre and 8 WT/AAV-Cre mice at 2 months after high dose of MA injection. KCl-evoked DA release was recorded in 150 striatal sites between 1.5 mm to 3.5 mm below the brain surface. Of these, 80 sites were taken from the striatum ipsilateral (L) to the AAV-Cre injection while 70 sites were recorded in the contralateral (R) striatum. Average dose of KCl ejected from micropipette was 176.9 +/− 7.5 nl per site. Local application of KCl resulted in release of dopamine in all striatal sites contralateral to AAV-Cre injection in both WT/AAV-Cre and loxP-PPARγ/AAV-Cre mice. Typical extracellular dopamine tracings from left and right striatum are shown in Fig 7A and 7B.

Previous voltammetric studies have shown a dose response relationship between the peak of extracellular DA level and log dose of applied DA through micropipette in rat striatum (Sabeti, J. et al., 2002a; Sabeti, J. et al., 2002b). In this study, the amplitude of DA release was thus normalized by comparing to the log volume (in nL) of KCl used. A similar approach has been used in our previous papers (Wang et al., 2003). We first examined the averaged KCl-evoked DA release in L or R striatum from all WT/AAV-Cre and loxP-PPARγ/AAV-Cre mice pretreated with high dose MA. There was a significant reduction in KCl-evoked DA release in the L striatum in the KO, as compared to R striatum in KO, L or R striatum in WT/AAV-Cre mice (Fig 8A, p<0.001, $F_{3,146}$= 7.713; p<0.001, post-hoc Newman-Keul test). No difference was found between the R and the L striata in WT/AAV-Cre mice. Previous studies have shown that KCl-evoked DA partially recovered after 1 month and fully recovered by 6 months after high doses of MA administration in adult Fisher rats (Cass and Manning, 1999). Similarly, no difference was found in the contralateral striatum between the animals treated with saline or MA at 2 months after injection. The rate of DA clearance (nM per sec) after KCl application was calculated between T20 and T60 as described previously (Cass and Manning, 1999). There was a significant reduction of DA clearance in the striatum ipsilateral to the AAV-Cre injection in loxP-PPARγ mice after MA treatment ($F_{3,137}$=3.826, P=0.011, one way ANOVA, Fig 8B).

KCl –evoked DA release and clearance were further analyzed topographically, every 0.5 mm, from 1.5 mm to 3.5 mm below the brain surface (Fig 9). The release of dopamine, elicited by KCl in the L striatum of loxP-PPARγ/AAV-Cre mice, was significantly reduced compared to the L striatum in WT/AAV-Cre mice (p<0.05, Two Way ANOVA + Newman Keuls test, Fig 9A). Most of these differences are found in dorsal striatum (Fig 9A). No difference was found in the R striatum between WT/AAV-Cre and loxP-PPARγ/AAV-Cre mice (Fig 9B). These data suggest that deficiency in PPARγ expression attenuates KCl - induced release of dopamine in the striatum. The reduction of DA clearance was mainly manifested in the left dorsal striatum in loxP-PPARγ/AAV-Cre (Fig 9C, p<0.05, 2 way ANOVA). No difference was found in the right striatum between WT/AAV-Cre and loxP-PPARγ/AAV-Cre mice (Fig 9D).

TH Immmunoreactivity

Mice receiving unilateral AAV-Cre were sacrificed after voltammetric recording or 2 months after MA or saline injection. AAV-Cre administration did not alter TH fiber or cell density in striatum or nigra in ipislateral, compared to the contralateral, hemisphere in 3 WT/AAV-Cre or in 3 loxP-PPARγ/AAV-Cre mice receiving saline injection. High dose of

MA treatment did not alter striatal TH immunoreactivity in WT/AAV-Cre mice (Fig 10-A); however, reduced TH immunoreactivity, mainly in the dorsal region, in loxP-PPARγ/AAV-Cre mice (Fig 10-B) was found. Striatal TH immunoreactivity of brain slices with an identified anterior commissure was further quantified using ImageJ. TH fiber density in left striatum, normalized to the TH activity in WT mice treated with saline, was significantly reduced in loxP-PPARγ/AAV-Cre (n=5), compared to WT/AAV-Cre (n=6), mice after MA injection (Fig 10-G, p=0.044, t test). In the midbrain area, administration of MA or saline did not affect TH immunoreactivity in the left nigra in WT/AAV-Cre mice (Figs 10-C and 10-E). In contrast, treatment with MA (Fig 10-D), but not saline (Fig 10-F), induced a prominent reduction in TH cell density in the left nigra area in loxP-PPARγ/AAV-Cre mice. The density of TH cells in midbrain slice between −3.16 mm and −3.64 mm from bregma was counted. TH cell count, ipislateral to the AAV-Cre injection side (left), were normalized to that on contralateral side (right) in each brain slice. A significantly reduction in TH cell count in left nigra (Fig 10-H, p=0.001, t test), but not in left VTA (Fig 10-I, p=0.980, t test), was found in loxP-PPARγ/AAV-Cre (n=7), compared to WT/AAV-Cre (n=5), mice receiving MA injection. No significant reduction in DAPI activity was found in left or right nigra region in these mice (p=0.185, $F_{3,16}$=1.815, one way ANOVA).

Discussion

In this study, we show that the GFP/Cre fusion protein is present in nigra, both in TH and non-TH cells one month after AAV-Cre injection. We found that administration of AAV-Cre caused reduction in PPARγ expression, detected by qRT-PCR, in nigra of loxP-PPARγ, but not WT/AAV-Cre, mice. Expression of GFP/Cre fusion protein using AAV serotype 7 in the midbrain was not limited to TH cells but did transduce approximately 56% of TH-immunoreactive cells in substantia nigra pars compacta. PCR analysis confirmed that recombination of the PPARγ gene occurred and caused a 50% reduction in PPARγ expression in the midbrain. Using immunostaining, we found a decrease of PPARγ -immunoreactivity in GFP/Cre-positive cells of loxP-PPARγ but not wild-type animals after AAV-Cre infection. These data suggest that administration of AAV-Cre provides a long term reduction of PPARγ expression in the substantia nigra of adult floxed animals. Our data support other reports that AAV serotype 7 transduces rodent neurons (Howard et al., 2008; Taymans et al., 2007). Taken together, these data suggest that local injection with AAV-Cre can deliver Cre recombinase, promote recombination, and cause a reduction of PPARγ expression in the TH neurons in nigra in the loxP-PPARγ mice.

It has been shown that activation of PPARγ by the exogenous agonist rosiglitazone prevents MPTP -mediated motor impairment and neurodegeneration in nigrostriatal dopaminergic neurons (Schintu et al., 2009). In this study, we examined the protective roles of endogenous PPARγ against dopaminergic toxicity induced by high doses of MA. We suppressed the endogenous PPARγ unilaterally in nigra by injection AAV-Cre to loxP-PPARγ mice to elicit rotational behavior, similar to that in the unilaterally 6-OHDA-lesion rodent model of Parkinson's disease. The imbalance in dopaminergic innervation after unilateral lesioning can be identified by rotation after injection of apomorphine or amphetamine (Ungerstedt and Arbuthnott, 1970) as well by rotarod without drug challenge (Fang et al., 2010; Monville et al., 2006; Rozas and Labandeira Garcia, 1997).

We found that administration of saline did not alter rotarod or rotational activity in WT/AAV-Cre or loxP-PPARγ/AAV-Cre mice. Similarly, KCl-evoked DA release or DA clearance in striatum was not altered in these animals (data not shown). These data suggest that the selective unilateral depletion of PPARγ alone does not alter DA release and clearance in striatum or locomotor function in the animals.

Both *in vivo* and *in vitro* studies have shown that high doses of MA acutely induces dysfunction in dopaminergic neurons, i.e. increasing apopototic markers, reducing tyrosine hydroxylase or DAT expression, and suppressing DA release (Chou et al., 2008; Shen et al., 2011). We also found that MA reduced TH immunoreactivity in striatum in both loxP - PPARγ and wild type mice receiving AAV-Cre. Our data suggest that high doses of MA can acutely induce neurodegeneration in striatum. Similar to rotarod behavioral responses on day 3 after MA administration, no difference in striatal TH activity was found between lox-P PPARγ/AAV-Cre and WT/AAV-Cre mice receiving MA. These data suggest that MA induces a similar neurodegeneration in these mice acutely after MA treatment.

A recent study has indicated that pretreatment with ibuprofen or the selective PPARγ agonist 15d-PG attenuates the reduction of striatal DAT expression after repeated MA injection (4mg/kg ×4) in mice (Tsuji et al., 2009), suggesting that activation of PPARγ by exogenous ligands attenuates MA toxicity. In this study, we found that unilaterally reducing PPARγ expression potentiated the MA –induced reduction in rotorod retention time, increased ipsilateral rotation after low dose MA injection, and lowered KCl-evoked DA release and clearance in the knock-out side striatum at 1–2 months after MA injection. Taken together, our data suggest that suppression of PPARγ potentiates MA –mediated toxicity in dopaminergic neurons.

Administration of amphetamine analogs causes ipislateral rotation in unilaterally 6-OHDA - lesioned rats due to differential increase of dopaminergic activity on the intact side. There is a correlation between amphetamine–induced ipislateral rotation and the depletion of dopamine in the nigra (Hudson et al., 1993). Unlike 6-OHDA –lesioned rats, which produces continuously and consistently ipislateral rotation after amphetamine administration, the floxed PPARγ and WT mice used in current study developed both ipislateral and contralateral rotations after administration of a low dose of MA. Such a difference may be due to (A) mice with C57/B6 background are more active in response to drug stimulation and/or (B) pretreatment with high doses of MA did not induce a near-complete lesioning in striatum comparable to 6-OHDA lesioning. Although these animals developed contra and ipsilateral rotation based on differential DA innervation between ipislateral and contra-lateral hemispheres, there was still a bias on direction of rotation. For example, no difference was found in contralateral rotation between WT/AAV-Cre and loxP-PPARγ/AAV-Cre mice, pretreated with either saline or high dose MA. A significant increase in ipislateral rotation was noted only in loxP-PPARγ/AAV-Cre pretreated with high dose of MA. The increase in ipislateral rotation suggests that high dose MA enhances degeneration of DA neurons unilaterally in loxP-PPARγ/AAV-Cre mice.

The deficiency in DA function in loxP-PPARγ/AAV-Cre mice at 2 months after MA treatment is further supported by in vivo electrochemical data. We used high speed chronoamperometry to examine the time course of KCl -evoked DA release and clearance in striatum. The dose of KCl applied locally was between $7–14 \times 10^{-11}$ mole (70 mM × 100 to 200 nl) per site. The dose, concentration and volume of the KCl solution have been previously reported to induce depolarization and release of dopamine at dopaminergic nerve terminals in vivo (Hoffman et al., 1998; Wang et al., 2003). We found that local administration of KCl induced DA release equally in L and R striatum of WT/AAV-Cre mice and in the non-viral injected striatum of loxP-PPARγ/AAV-Cre mice. Previous studies have demonstrated that the suppression of KCl-mediated DA release is reversible in 1 to 6 months after high doses of MA administration in adult Fisher rats (Cass and Manning, 1999), suggesting a spontaneous recovery of DA release function. We also found no difference in DA release between MA and saline –treated WT/AAV-Cre mice at 2 months after injection. In contrast to saline injection, KCl-evoked DA release and the rate of DA clearance were significantly attenuated in the L striatum in loxP-PPARγ/AAV-Cre at 2

months after MA treatment. These electrochemical data suggest that deficiency in PPARγ expression in nigra potentiates or prolongs MA-mediated neurodegeneration in striatum. In agreement with changes in distribution of TH immunoreactivity, the suppression of KCl-evoked DA release and clearance in the loxP-PPARγ/AAV-Cre mice was mainly seen in the dorsal striatum. Less difference between loxP-PPARγ/AAV-Cre and WT/AAV-Cre was found in the ventral striatum, which may be attributed to its topographic innervation of dopaminergic neurons from VTA.

We have previously demonstrated that MA binge treatment (10mg/kg ×4) does not lead to loss of dopaminergic neurons in SNpc (Luo et al., 2010). There is a significant reduction of TH immunoreactivity in striatum at 3 days after MA treatment (Chou et al., 2008), suggesting that MA produced mainly DA terminal lesions. In this study, we found that deficiency in PPARγ expression can lead to a chronic reduction of TH cell bodies in ipislateral nigra after binge MA treatment, suggesting that suppression PPARγ expression reduces protection in nigra after MA treatment.

Several reports have supported that PPARγ exerts protective effects through anti-inflammation. PPARγ agonists inhibited production of monocyte inflammatory cytokines (Jiang et al., 1998). Treatment with the PPARγ agonist pioglitazone reduced MPTP-mediated microglia activation and neurotoxicity in nigral dopaminergic neurons (Dehmer et al., 2004). On the other hand, high dose of MA induced inflammation (Asanuma et al., 2004). It is thus possible that deficiency in endogenous PPARγ may indirectly facilitate MA-mediated inflammatory reactions, which may result in regional neurodegeneration in mice with unilateral depletion of PPARγ. Further studies are needed to determine the role of inflammation in MA-mediated midbrain toxicity in these animals.

In summary, our behavioral, histological and electrochemical data suggest that deficiency in endogenous PPARγ does not alter dopaminergic function in the absence of injury, but enhances neurodegeneration after exposure to high dose MA. It has been reported that endogenous PPARγ expression is suppressed in certain clinical disorders (Hindle et al., 2009; Yamamoto-Furusho et al., 2010) and can be inhibited by various pharmacological agents. It may be that a deficiency in endogenous PPARγ in these or other conditions increases vulnerability to MA insults and that endogenous PPARγ may play an important role in reducing MA toxicity in vivo. Moreover, one recent study has indicated that conditionally knocking out PPARγ increases ischemic brain damage (Zhao et al., 2009). These data supports the idea that PPARγ is important for minimizing brain injury and may be a target for pharmacotherapy in neurodegeneration.

Acknowledgments

This study was supported by NIDA IRP. We thank Dr. Barry Hoffer for his critical suggestions.

List of abbreviations

AAV	adeno-associated virus
DAPI	4’, 6-diamidino-2-phenylindole
DA	dopamine
ETime	endurance times
GFP	green fluorescent protein
GFP/Cre	GFP-Cre fusion protein

KO	knockout
MA	methamphetamine
PPARγ	peroxisome proliferator-activated receptor gamma
PPRE	PPAR response element
RXR	retinoic X receptor
TH	tyrosine hydroxylase
WT	wild type

References

Asanuma M, Miyazaki I, Higashi Y, Tsuji T, Ogawa N. Specific gene expression and possible involvement of inflammation in methamphetamine-induced neurotoxicity. Ann. NY. Acad. Sci. 2004; 1025:69–75. [PubMed: 15542702]

Barak Y, Nelson MC, Ong ES, Jones YZ, Ruiz-Lozano P, Chien KR, Koder A, Evans RM. PPAR gamma is required for placental, cardiac, and adipose tissue development. Mol. Cell. 1999; 4:585–595. [PubMed: 10549290]

Cass WA, Manning MW. Recovery of presynaptic dopaminergic functioning in rats treated with neurotoxic doses of methamphetamine. J. Neurosci. 1999; 19:7653–7660. [PubMed: 10460271]

Chou J, Luo Y, Kuo CC, Powers K, Shen H, Harvey BK, Hoffer BJ, Wang Y. Bone morphogenetic protein-7 reduces toxicity induced by high doses of methamphetamine in rodents. Neuroscience. 2008; 151:92–103. [PubMed: 18082966]

Dehmer T, Heneka MT, Sastre M, Dichgans J, Schulz JB. Protection by pioglitazone in the MPTP model of Parkinson's disease correlates with I kappa B alpha induction and block of NF kappa B and iNOS activation. J. Neurochem. 2004; 88:494–501. [PubMed: 14690537]

Fang X, Sugiyama K, Akamine S, Sun W, Namba H. The different performance among motor tasks during the increasing current intensity of deep brain stimulation of the subthalamic nucleus in rats with different degrees of the unilateral striatal lesion. Neurosci. Lett. 2010; 480:64–68. [PubMed: 20573573]

Gao GP, Alvira MR, Wang L, Calcedo R, Johnston J, Wilson JM. Novel adeno-associated viruses from rhesus monkeys as vectors for human gene therapy. Proc. Natl. Acad. Sci. U. S. A. 2002; 99:11854–11859. [PubMed: 12192090]

Grace CE, Schaefer TL, Herring NR, Graham DL, Skelton MR, Gudelsky GA, Williams MT, Vorhees CV. Effect of a neurotoxic dose regimen of (+)-methamphetamine on behavior, plasma corticosterone, and brain monoamines in adult C57BL/6 mice. Neurotoxicol. Teratol. 2010; 32:346–355. [PubMed: 20096350]

He W, Barak Y, Hevener A, Olson P, Liao D, Le J, Nelson M, Ong E, Olefsky JM, Evans RM. Adipose-specific peroxisome proliferator-activated receptor gamma knockout causes insulin resistance in fat and liver but not in muscle. Proc. Natl. Acad. Sci. U. S. A. 2003; 100:15712–15717. [PubMed: 14660788]

Hindle AK, Koury J, McCaffrey T, Fu SW, Brody F. Dysregulation of gene expression within the peroxisome proliferator activated receptor pathway in morbidly obese patients. Surg. Endosc. 2009; 23:1292–1297. [PubMed: 18855061]

Hoffman AF, Lupica CR, Gerhardt GA. Dopamine transporter activity in the substantia nigra and striatum assessed by high-speed chronoamperometric recordings in brain slices. J. Pharmacol. Exp. Ther. 1998; 287:487–496. [PubMed: 9808671]

Howard DB, Powers K, Wang Y, Harvey BK. Tropism and toxicity of adeno-associated viral vector serotypes 1,2,5,6,7,8,9 in rat neurons and glia *in vitro*. Virology. 2008; 372:24–34. [PubMed: 18035387]

Hudson JL, van Horne CG, Stromberg I, Brock S, Clayton J, Masserano J, Hoffer BJ, Gerhardt GA. Correlation of apomorphine- and amphetamine-induced turning with nigrostriatal dopamine

content in unilateral 6-hydroxydopamine lesioned rats. Brain Res. 1993; 626:167–174. [PubMed: 8281427]

Isaac AO, Kawikova I, Bothwell AL, Daniels CK, Lai JC. Manganese treatment modulates the expression of peroxisome proliferator-activated receptors in astrocytoma and neuroblastoma cells. Neurochem. Res. 2006; 31:1305–1316. [PubMed: 17053972]

Jayanthi S, Deng X, Ladenheim B, McCoy MT, Cluster A, Cai NS, Cadet JL. Calcineurin/NFAT-induced up-regulation of the Fas ligand/Fas death pathway is involved in methamphetamine-induced neuronal apoptosis. Proc. Natl. Acad. Sci. U. S. A. 2005; 102:868–873. [PubMed: 15644446]

Jiang C, Ting AT, Seed B. PPAR-gamma agonists inhibit production of monocyte inflammatory cytokines. Nature. 1998; 391:82–86. [PubMed: 9422509]

Jiang Q, Heneka M, Landreth GE. The role of peroxisome proliferator-activated receptor-gamma (PPARgamma) in Alzheimer's disease: therapeutic implications. CNS. Drugs. 2008; 22:1–14. [PubMed: 18072811]

Kaspar BK, Vissel B, Bengoechea T, Crone S, Randolph-Moore L, Muller R, Brandon EP, Schaffer D, Verma IM, Lee KF, Heinemann SF, Gage FH. Adeno-associated virus effectively mediates conditional gene modification in the brain. Proc. Natl. Acad. Sci. U. S. A. 2002; 99:2320–2325. [PubMed: 11842206]

Kobayashi MS, Takahashi Y, Nagata T, Nishida Y, Murata A, Ishikawa K, Asai S. Screening for control genes in rat global cerebral ischemia using high-density oligonucleotide array. J. Neurosci. Res. 2004; 76:512–518. [PubMed: 15114623]

Lowery RL, Zhang Y, Kelly EA, Lamantia CE, Harvey BK, Majewska AK. Rapid, long-term labeling of cells in the developing and adult rodent visual cortex using double-stranded adeno-associated viral vectors. Dev. Neurobiol. 2009; 69:674–688. [PubMed: 19551873]

Luo Y, Wang Y, Kuang SY, Chiang YH, Hoffer BJ. Decreased level of Nurr1 in heterozygous young adult mice leads to exacerbated acute and long-term toxicity after repeated methamphetamine exposure. PLoS. One. 2010; 5:e15193. [PubMed: 21151937]

Maeda T, Kiguchi N, Fukazawa Y, Yamamoto A, Ozaki M, Kishioka S. Peroxisome proliferator-activated receptor gamma activation relieves expression of behavioral sensitization to methamphetamine in mice. Neuropsychopharmacology. 2007; 32:1133–1140. [PubMed: 17019405]

Monville C, Torres EM, Dunnett SB. Comparison of incremental and accelerating protocols of the rotarod test for the assessment of motor deficits in the 6-OHDA model. J. Neurosci. Methods. 2006; 158:219–223. [PubMed: 16837051]

Quinn LP, Crook B, Hows ME, Vidgeon-Hart M, Chapman H, Upton N, Medhurst AD, Virley DJ. The PPARgamma agonist pioglitazone is effective in the MPTP mouse model of Parkinson's disease through inhibition of monoamine oxidase B. Br. J Pharmacol. 2008; 154:226–233. [PubMed: 18332857]

Rozas G, Labandeira Garcia JL. Drug-free evaluation of rat models of parkinsonism and nigral grafts using a new automated rotarod test. Brain Res. 1997; 749:188–199. [PubMed: 9138718]

Sabeti J, Adams CE, Burmeister J, Gerhardt GA, Zahniser NR. Kinetic analysis of striatal clearance of exogenous dopamine recorded by chronoamperometry in freely-moving rats. J. Neurosci. Methods. 2002a; 121:41–52. [PubMed: 12393160]

Sabeti J, Gerhardt GA, Zahniser NR. Acute cocaine differentially alters accumbens and striatal dopamine clearance in low and high cocaine locomotor responders: behavioral and electrochemical recordings in freely moving rats. J. Pharmacol. Exp. Ther. 2002b; 302:1201–1211. [PubMed: 12183681]

Scammell TE, Arrigoni E, Thompson MA, Ronan PJ, Saper CB, Greene RW. Focal deletion of the adenosine A1 receptor in adult mice using an adeno-associated viral vector. J Neurosci. 2003; 23:5762–5770. [PubMed: 12843280]

Schintu N, Frau L, Ibba M, Caboni P, Garau A, Carboni E, Carta AR. PPAR-gamma-mediated neuroprotection in a chronic mouse model of Parkinson's disease. Eur. J Neurosci. 2009; 29:954–963. [PubMed: 19245367]

Schmittgen TD, Livak KJ. Analyzing real-time PCR data by the comparative C(T) method. Nat. Protoc. 2008; 3:1101–1108. [PubMed: 18546601]

Shen H, Luo Y, Yu SJ, Wang Y. Enhanced neurodegeneration after a high dose of methamphetamine in adenosine A3 receptor null mutant mice. Neuroscience. 2011; 194:170–180. [PubMed: 21867746]

Shimazu T, Inoue I, Araki N, Asano Y, Sawada M, Furuya D, Nagoya H, Greenberg JH. A peroxisome proliferator-activated receptor-gamma agonist reduces infarct size in transient but not in permanent ischemia. Stroke. 2005; 36:353–359. [PubMed: 15618443]

Taymans JM, Vandenberghe LH, Haute CV, Thiry I, Deroose CM, Mortelmans L, Wilson JM, Debyser Z, Baekelandt V. Comparative analysis of adeno-associated viral vector serotypes 1, 2, 5, 7, and 8 in mouse brain. Hum. Gene Ther. 2007; 18:195–206. [PubMed: 17343566]

Tsuji T, Asanuma M, Miyazaki I, Miyoshi K, Ogawa N. Reduction of nuclear peroxisome proliferator-activated receptor gamma expression in methamphetamine-induced neurotoxicity and neuroprotective effects of ibuprofen. Neurochem. Res. 2009; 34:764–774. [PubMed: 18946735]

Tureyen K, Kapadia R, Bowen KK, Satriotomo I, Liang J, Feinstein DL, Vemuganti R. Peroxisome proliferator-activated receptor-gamma agonists induce neuroprotection following transient focal ischemia in normotensive, normoglycemic as well as hypertensive and type-2 diabetic rodents. J Neurochem. 2007; 101:41–56. [PubMed: 17394460]

Ungerstedt U, Arbuthnott GW. Quantitative recording of rotational behavior in rats after 6- hydroxy-dopamine lesions of the nigrostriatal dopamine system. Brain Res. 1970; 24:485–493. [PubMed: 5494536]

Victor NA, Wanderi EW, Gamboa J, Zhao X, Aronowski J, Deininger K, Lust WD, Landreth GE, Sundararajan S. Altered PPARgamma expression and activation after transient focal ischemia in rats. Eur. J. Neurosci. 2006; 24:1653–1663. [PubMed: 17004929]

Wang Y, Chang CF, Morales M, Chiang YH, Harvey BK, Su TP, Tsao LI, Chen SY, Thiemermann C. Diadenosine tetraphosphate protects against injuries induced by ischemia and 6-hydroxydopamine in rat brain. J. Neurosci. 2003; 23:7958–7965. [PubMed: 12944527]

Wang Y, Hayashi T, Chang CF, Chiang YH, Tsao LI, Su TP, Borlongan CV, Lin SZ. Methamphetamine potentiates ischemia/reperfusion insults after transient middle cerebral artery ligation. Stroke. 2001; 32:775–782. [PubMed: 11239201]

Xiao X, Li J, Samulski RJ. Production of high-titer recombinant adeno-associated virus vectors in the absence of helper adenovirus. J. Virol. 1998; 72:2224–2232. [PubMed: 9499080]

Xu YW, Sun L, Liang H, Sun GM, Cheng Y. 12/15-Lipoxygenase inhibitor baicalein suppresses PPAR gamma expression and nuclear translocation induced by cerebral ischemia/reperfusion. Brain Res. 2010; 1307:149–157. [PubMed: 19853588]

Yamamoto-Furusho JK, Penaloza-Coronel A, Sanchez-Munoz F, Barreto-Zuniga R, Dominguez-Lopez A. Peroxisome proliferator-activated receptor-gamma (PPAR-gamma) expression is downregulated in patients with active ulcerative colitis. Inflamm. Bowel. Dis. 2010 In Press.

Zhao X, Strong R, Zhang J, Sun G, Tsien JZ, Cui Z, Grotta JC, Aronowski J. Neuronal PPARgamma deficiency increases susceptibility to brain damage after cerebral ischemia. J Neurosci. 2009; 29:6186–6195. [PubMed: 19439596]

Zhao Y, Patzer A, Gohlke P, Herdegen T, Culman J. The intracerebral application of the PPARgamma-ligand pioglitazone confers neuroprotection against focal ischaemia in the rat brain. Eur. J Neurosci. 2005; 22:278–282. [PubMed: 16029218]

Zhou FC, Chiang YH, Wang Y. Constructing a new nigrostriatal pathway in the Parkinsonian model with bridged neural transplantation in substantia nigra. J. Neurosci. 1996; 16:6965–6974. [PubMed: 8824333]

Zhu JP, Xu W, Angulo N, Angulo JA. Methamphetamine-induced striatal apoptosis in the mouse brain: comparison of a binge to an acute bolus drug administration. Neurotoxicology. 2006; 27:131–136. [PubMed: 16165214]

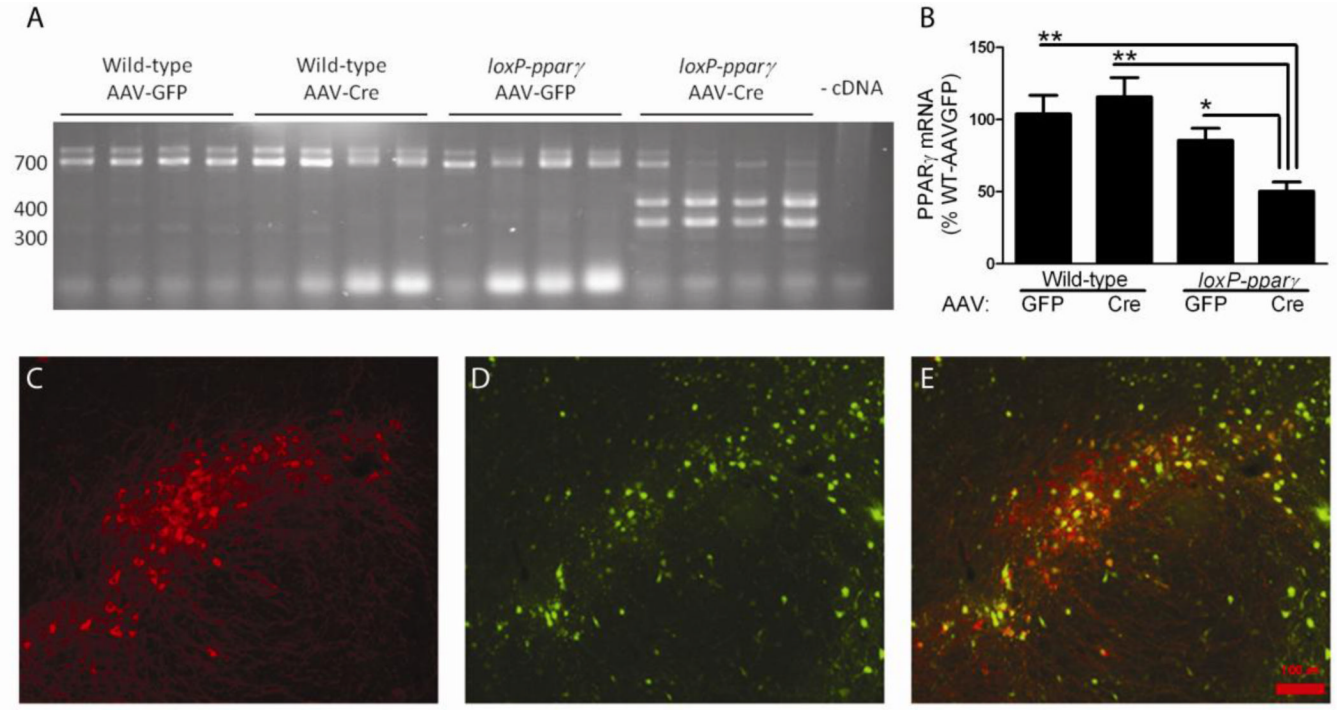

Fig 1.

AAV-Cre delivery to midbrain of loxP-PPARγ mice causes recombination with the PPARγ gene and a 50% reduction in PPARγ mRNA expression. A) Recombination of PPARγ only detected in loxP-PPARγ mice that received AAV-Cre. Male C57/Bl6 (wild-type) or PPARγ mice were bilaterally injected into midbrain with either AAV-GFP or AAV-Cre virus (1×10^10 vg/site). Recombination was only detected in cDNA from loxP-PPARγ animals using a qualitative PCR assay that yields either wild-type (700 bp) and recombinant PPARγ (300 and 400 bp, representing splice variants) on an ethidium stained agarose gel. Each lane represents one animal. B) Real-time PCR of cDNA revealed that only loxP-PPARγ animals receiving AAV-Cre showed a significant reduction in PPARγ (~50%). Data was normalized to reference gene, Ube2i. *p<0.05, **p<0.01, One-way ANOVA, Newman-Keuls post-hoc analysis compared to WT/AAV-GFP group. C–E) Tyrosine hydroxylase immunoreactivity (C), GFP fluorescence (D), and merged image (E) at 2 weeks after local administration of AAV-GFP/Cre injection in nigra region. GFP was detected in both TH-positive and TH-negative cells.

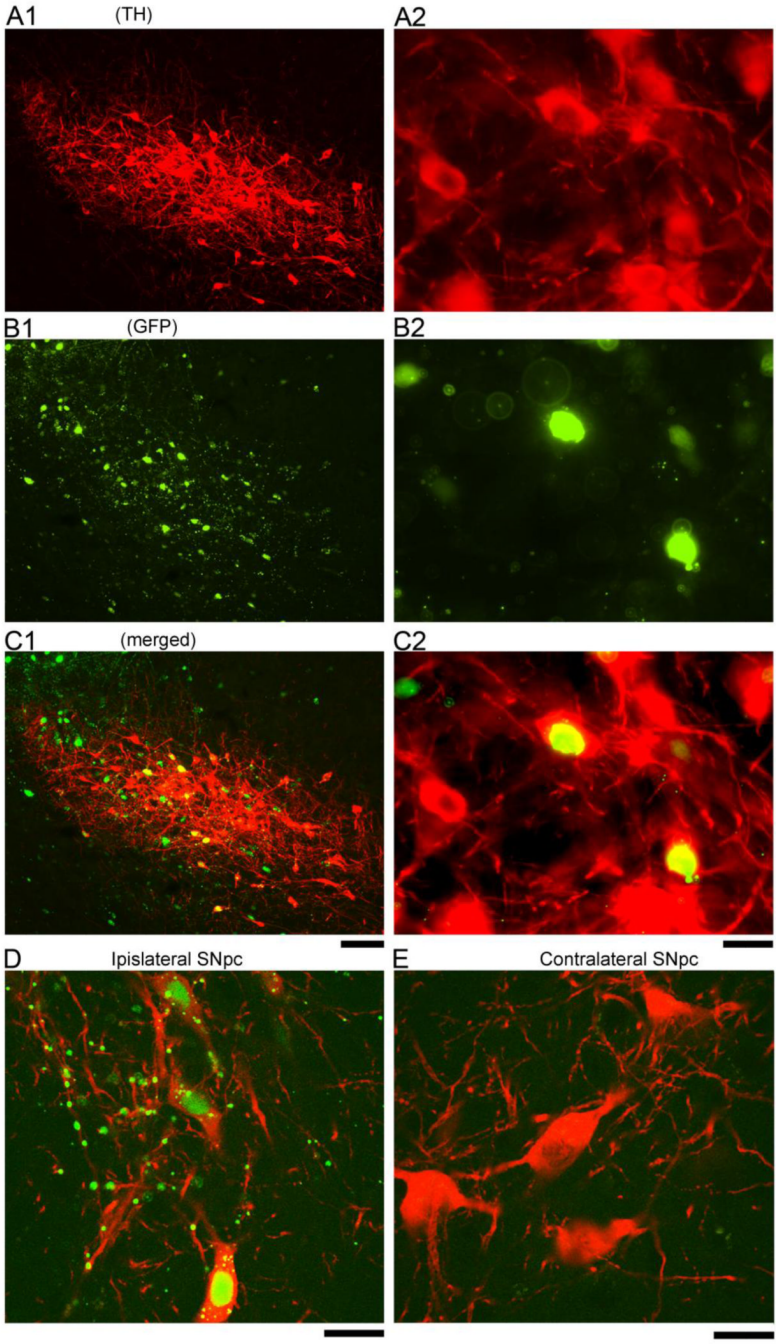

Fig 2.

The GFP/Cre fusion protein of AAV-Cre is expressed in dopaminergic and non-dopaminergic cells in nigra at one month after AAV-Cre injection. TH immunoreactivity (A1 & A2, low and high magnification) and GFP fluorescence (B1 & B2) were found in the nigra area at the site of injection. GFP fluorescence was co-expressed in TH (B1 & B2) and non-TH cells in nigra (C1 & C2, merged). Confocal photomicrographs indicate that GFP/Cre is present in the nuclei of TH containing cells in substantia nigra pars compacta (SNpc), ipislateral to AAV-Cre injection (D). No GFP fluorescence was observed in the TH cells in the contralateral SNpc (E). Scale Bar: A1, B1, C1: 100 μm; A2, B2, C2, D, E: 20 μm.

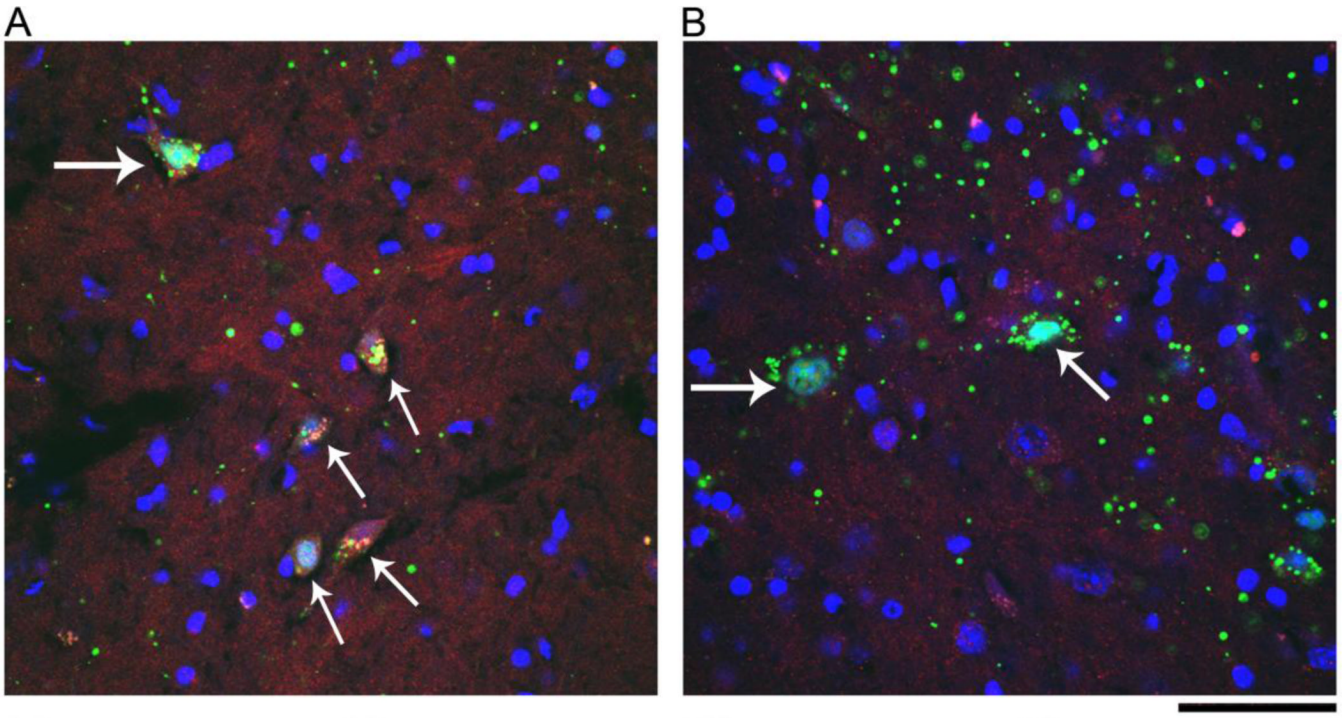

Fig 3.

Injection of AAV-Cre reduces PPARγ expression in the nigra region in floxed PPARγ mice. (A) Both PPARγ (red) and GFP (green) were expressed in the same cells (arrows) in nigra area at 2 months after injection of AAV-Cre to a wild type mouse. (B) PPARγ immunoreactivity was suppressed in cells expressed GFP (arrows) after injection of AAV-Cre to a floxed PPARγ mouse. Scale bar = 50 μm.

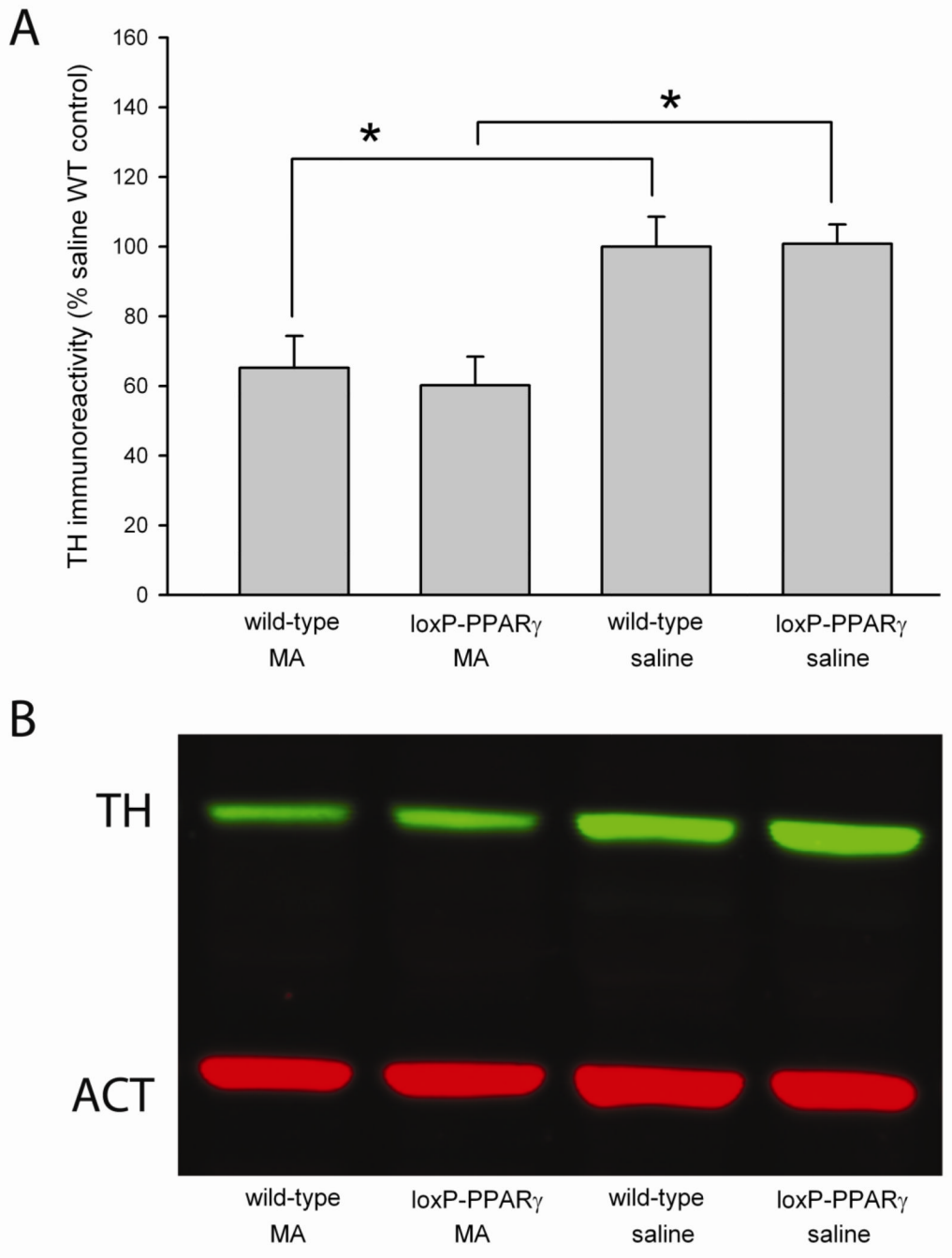

Fig 4.

Acute MA treatment reduces TH immunoreactivity in lox-P PPARγ/AAV-Cre or WT/AAV-Cre mice. WT and loxP-PPARγ mice were treated with AAV-Cre unilaterally in left nigra area. Striatal tissue in left hemisphere was collected for Western analysis at 2 days after administration of MA or saline. (A) MA treatment significantly reduced striatal TH/actin immunoreactivity in loxP-PPARγ/AAV-Cre and WT/AAV-Cre mice. *p<0.05, 2-way ANOVA. (B) An example of TH and actin Western blotting from mice receiving MA or saline.

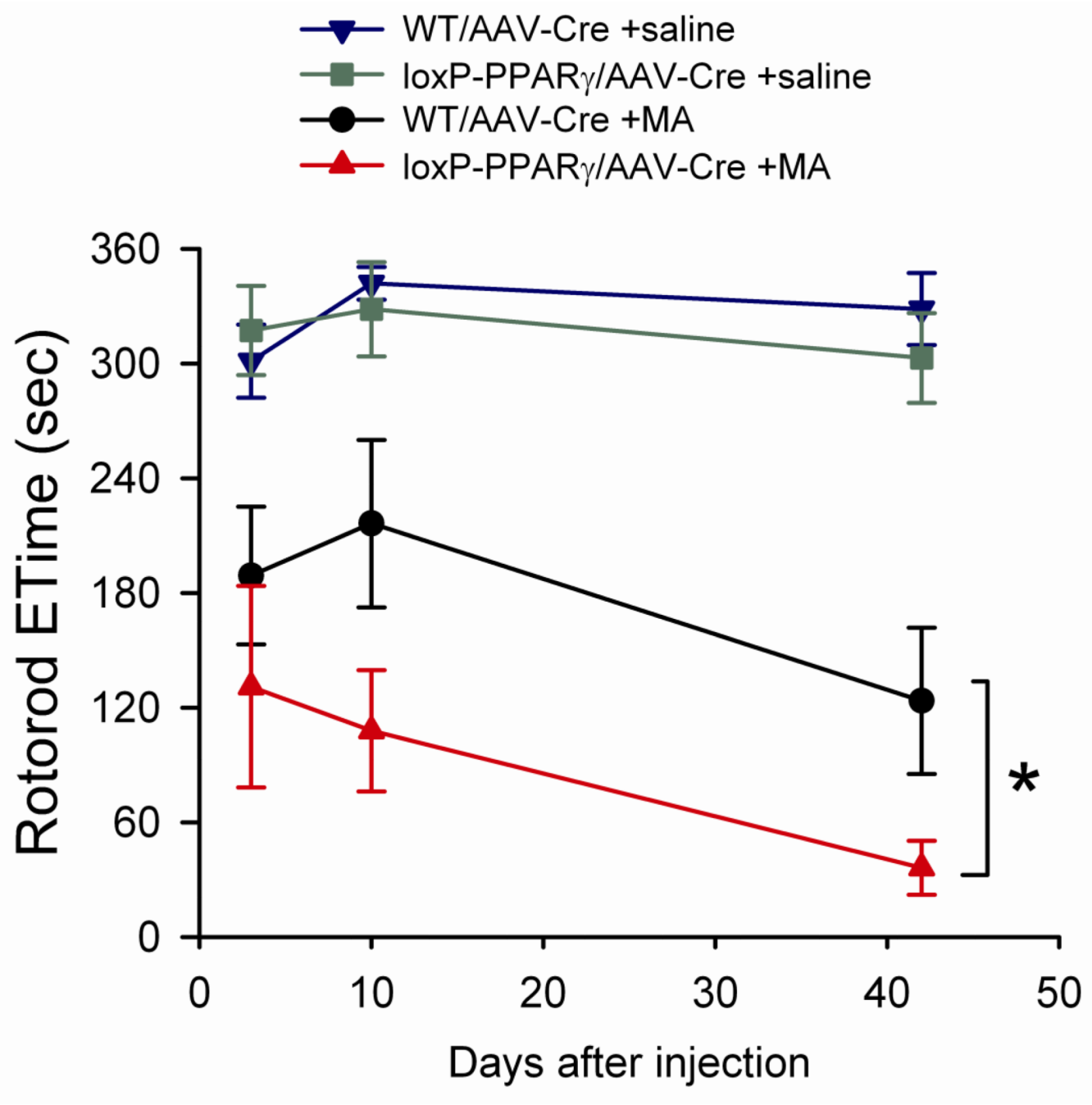

Fig 5.

Methamphetamine pretreatment reduced endurance times (ETime) on the rotarod in loxP-PPARγ/AAV-Cre mice. Fifteen loxP-PPARγ/AAV-Cre and 18 WT/AAV-Cre mice were treated with MA (10 mg/kg ×4) or saline on day 0. Rotorod tests were taken on day 3, 10 and 42 after injection. Pretreatment with MA significantly reduced Etime. There is a further reduction of Etime in loxP-PPARγ/AAV-Cre, compared to WT/AAV-Cre, mice. *$p<0.05$, 3-Way ANOVA+Newman Keuls test.

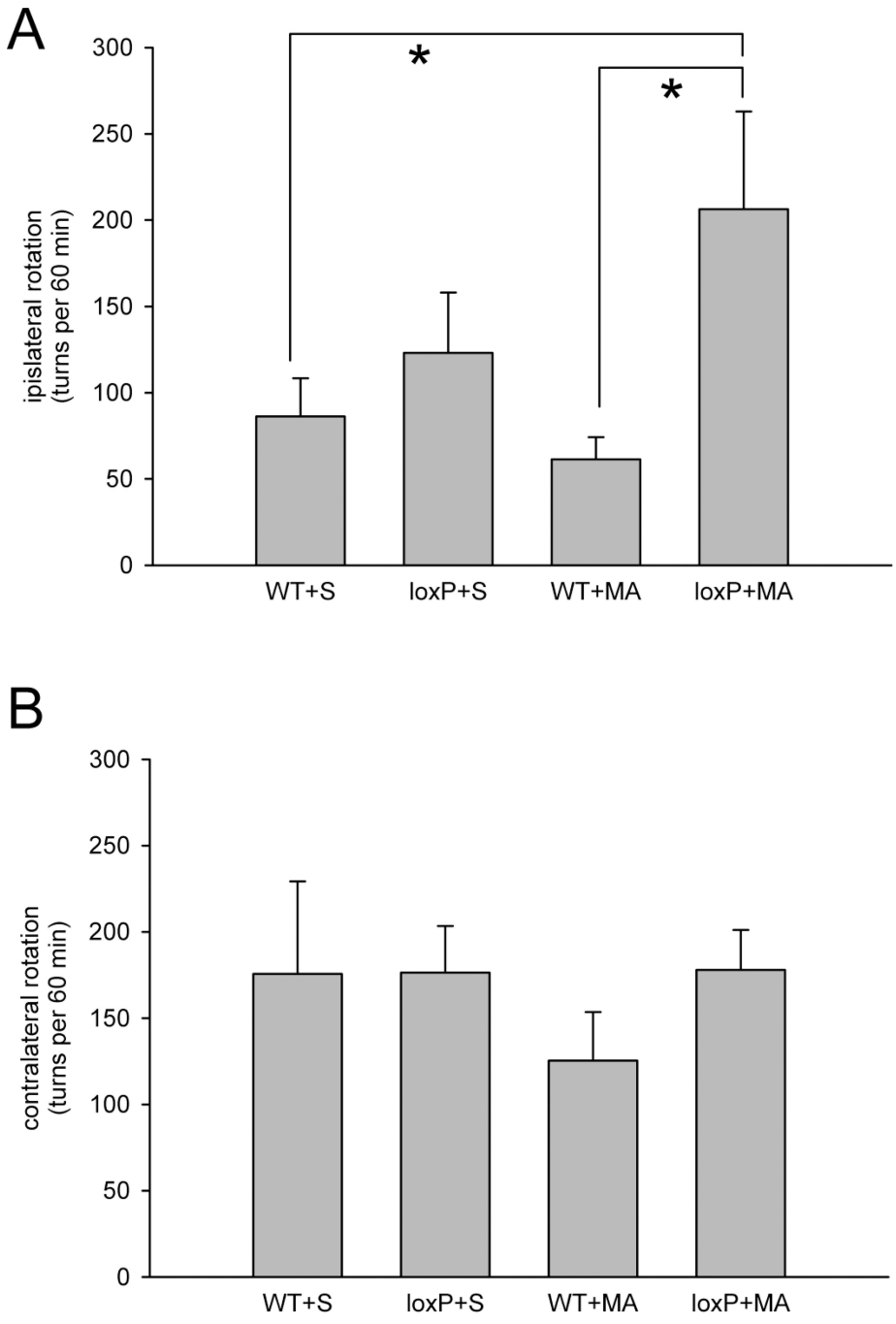

Fig 6.

(A) Increase in ipislateral rotation in loxP-PPARγ/AAV-Cre mice previously exposed to high dose of MA (10mg/kg ×4). At 45 days after receiving saline or high dose of MA, animals were challenged with a low dose MA (2.5 mg/kg, s.c.) to induced rotation. There is a significant increase in ipislateral rotation in the loxP-PPARγ/AAV-Cre mice that previously received high dose MA ($p<0.05$, two way ANOVA). (B) No difference was found in the contralateral rotation between loxP-PPARγ/AAV-Cre and WT/AAV-Cre mice receiving treatment with saline or with high dose of MA ($p=0.963$, two way ANOVA).

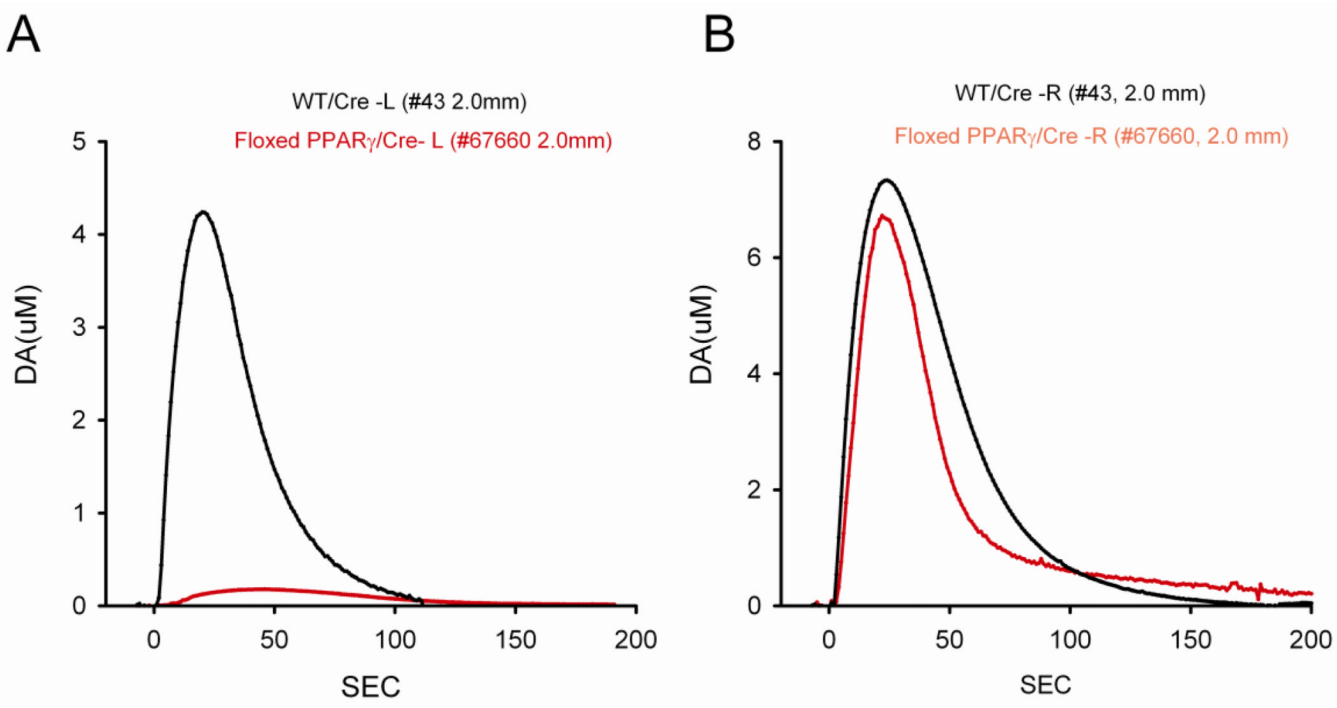

Fig 7.

Typical voltammetric tracings of extracellular DA concentration in dorsal striatum in animals previously exposed to high doses of MA. KCl –evoked dopamine release was obtained from striatum at 2 mm below brain surface ipsilateral (A) or contralateral (B) to AAV-Cre injection. KCl was delivered locally through a micropipette next to DA sensor at time 0. (A) KCl -mediated DA release was greatly suppressed in the left striatum in loxP-PPAR**γ**/AAV-Cre mouse (red tracing from mouse #67660), compared to WT/AAV-Cre mouse (black tracing from mouse #43). (B) No difference in DA release was found in the right striatum between WT/AAV-Cre (black tracing from mouse #43) and loxP-PPAR**γ**/AAV-Cre (red tracing from mouse #67660) mice.

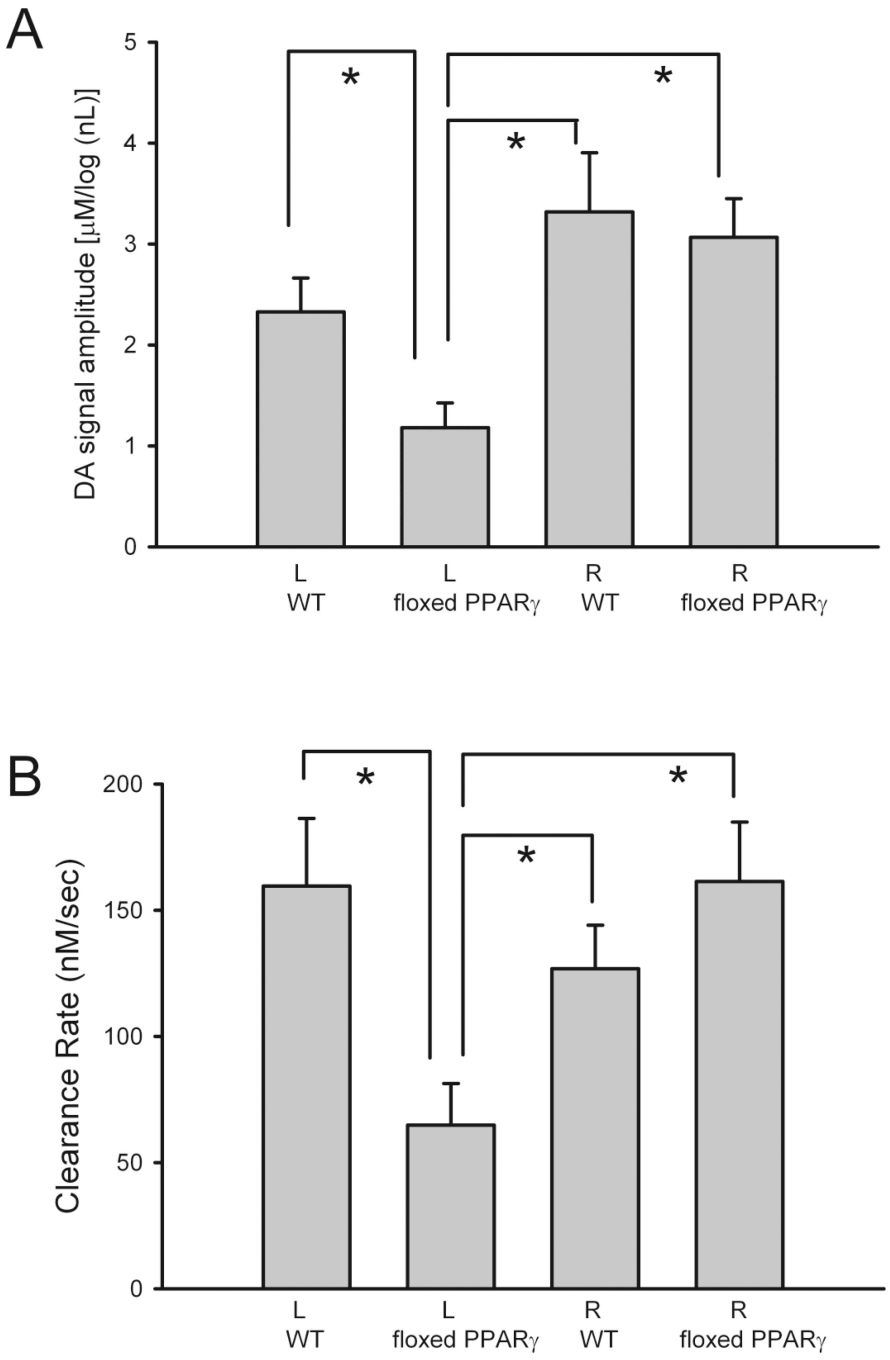

Fig 8.

Averaged DA release (A) and rate of DA clearance (B) were significantly reduced in left (L) striatum in loxP-PPARγ/AAV-Cre mice pretreated with high dose MA. (A) The peak amplitude of the DA signal, induced by local KCl administration, was averaged in L or R striatum of WT/AAV-Cre and loxP-PPARγ/AAV-Cre mice. There is a significant reduction of KCl-evoked DA release in the L striatum in KO, as compared to R striatum in KO, and to L or R striata in WT/AAV-Cre mice ($p<0.001$). (B) The rate of DA clearance (nM per sec) after KCl application was calculated between T20 and T60. There is a significant reduction in DA clearance in the striatum ipislateral to the AAV-Cre injection in loxP-PPARγ mice after MA treatment ($p=0.011$, one way ANOVA).

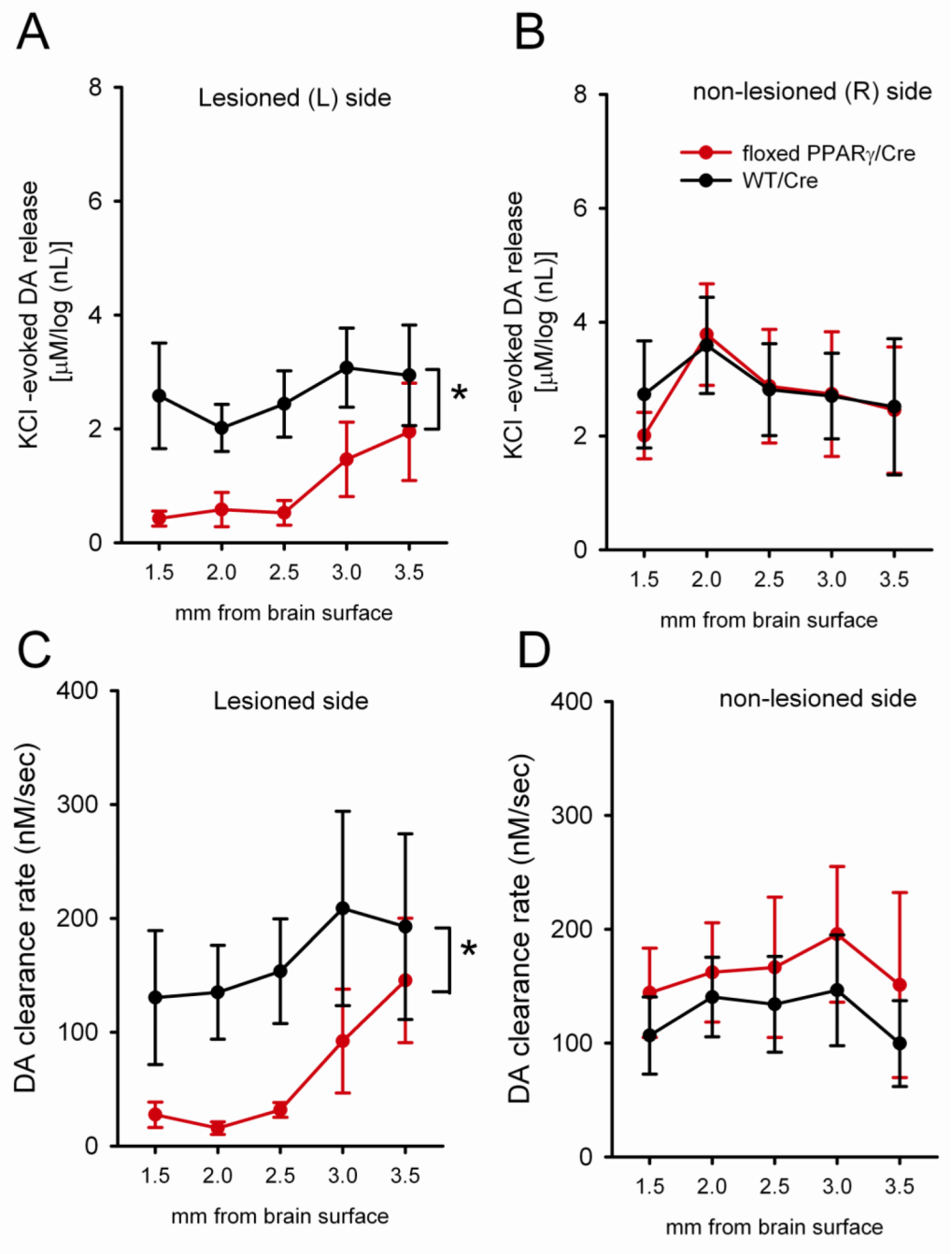

Fig 9.

Topographic distribution of (A, B) KCl –evoked DA release and (C, D) clearance in the striatum in loxP-PPARγ/AAV-Cre (red tracing) and WT/AAV-Cre (black tracing) at 2 months after high dose MA administration. (A) The release of dopamine elicited by KCl in the L striatum of mice was significantly reduced, compared to the L striatum in WT/AAV-Cre mice ($p<0.05$, two way ANOVA + Newman-Keuls test). Most of these differences were in dorsal striatum. (B) No difference was found in the R striatum between WT/AAV-Cre and loxP-PPARγ/AAV-Cre mice. (C) A reduction in DA clearance was seen in the L striatum in loxP-PPARγ/AAV-Cre mice ($p<0.05$, two way ANOVA). (D) No difference in

clearance was found in the contralateral striatum between WT/AAV-Cre and loxP-PPARγ/AAV-Cre mice.

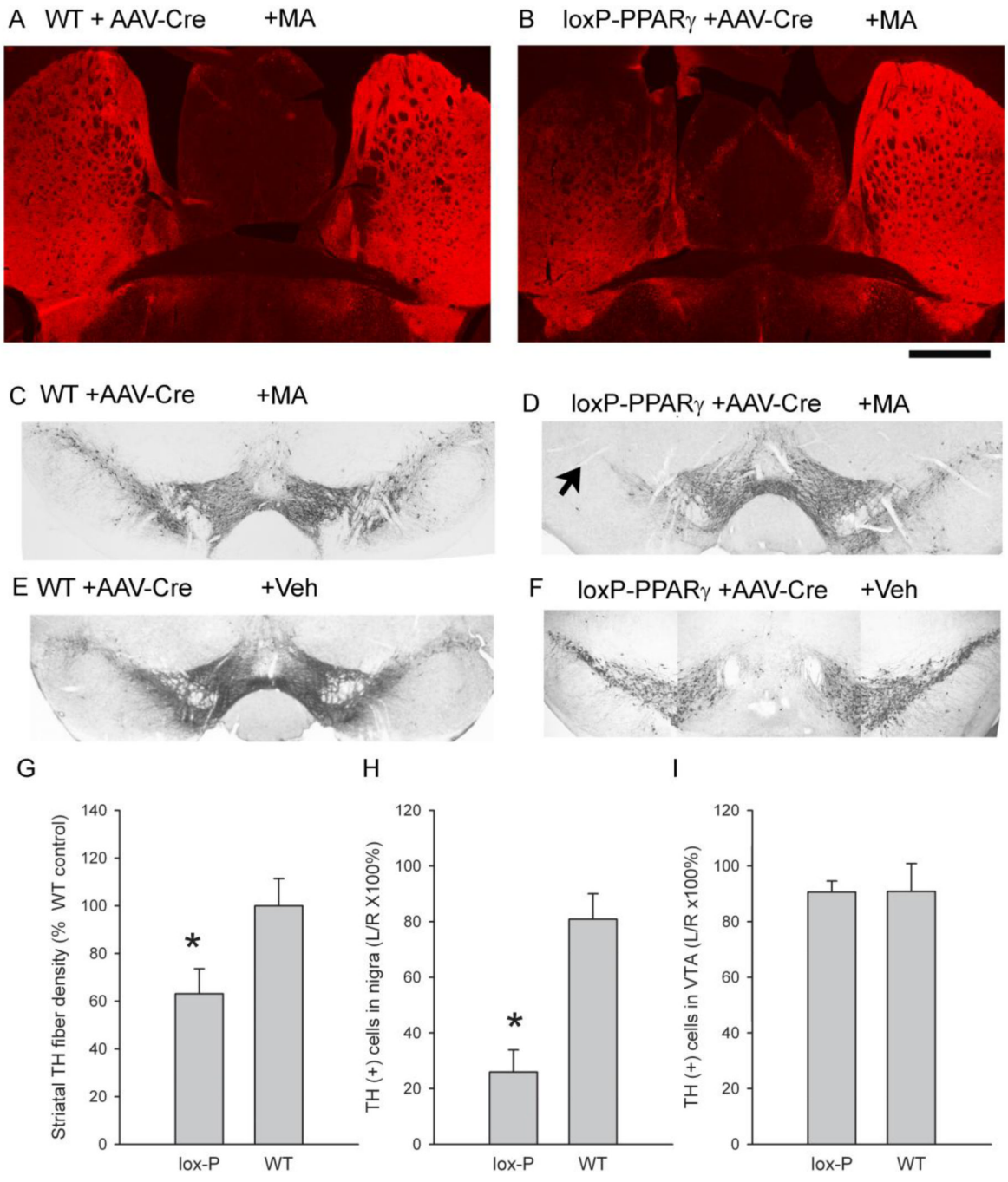

Fig 10.

Reduction of TH immunoreactivity in loxP-PPARγ/AAV-Cre mice at 2 months after MA injection. (A, C) In a wild type animal, unilateral injection AAV-Cre to the left nigra area did not alter TH immunoreactivity at 2 months after MA injection in (A) striatum and (C) nigra, ipsilateral to AAV-Cre injection. In contrast, in a loxP-PPARγ mouse (B & D), MA treatment reduced TH immunoreactivity in the (B) left striatum and (D) left nigra region (arrow), ipislateral to AAV-Cre injection. Administration of saline did not alter TH activity in nigra region in (E) WT and (F) loxP-PPARγ mice. Scale bar: A, B: 1 mm. (G) TH fiber density in left striatum at the level of anterior commissure, normalized to striatal TH density in WT mice treated with saline, was significantly reduced in loxP-PPARγ/AAV-Cre,

compared to WT/AAV-Cre, mice after MA injection (p=0.044, t test). (H and I) TH cell counts, ipislateral to the AAV-Cre injection side (left), were normalized to that in contralateral side (right) in each brain slice. A significant reduction in TH cell counts in left nigra (H, p=0.001, t test), but not in left VTA (I, p=0.980, t test), was found in loxP-PPARγ/AAV-Cre, compared to WT/AAV-Cre, mice receiving MA injection.